Development of empirical bond-order-type interatomic potential for amorphous carbon structures

T. Kumagai,[a] S. Hara, J. Choi, S. Izumi, and T. Kato
School of Engineering, The University of Tokyo, 7-3-1, Hongo, Bunkyo-ku, Tokyo 113-8656, Japan

(Received 10 October 2008; accepted 17 January 2009; published online 19 March 2009)

A bond-order-type interatomic potential has been developed for reproducing amorphous carbon (*a*-C) structures. Several improvements have been incorporated into the conventional Brenner potential so that the material properties of carbon crystals remain unchanged. The main characteristics of the potential function developed in the present research are the use of a screening function instead of a cutoff function and the introduction of a dihedral angle potential around the bond between two threefold coordinated atoms. By using the developed interatomic potential, we can reproduce the material properties of *a*-C structures, such as the fraction of sp^3-bonded atoms, radial distribution function, and ring statistics. It is found that the correction term enhances the formation of cluster structures in *a*-C, which is confirmed in the first-principles calculation. © *2009 American Institute of Physics*. [DOI: 10.1063/1.3086631]

I. INTRODUCTION

Diamondlike carbon (DLC) films are well known for their low friction coefficient and excellent corrosion resistance and wear resistance.[1] A DLC film is an amorphous carbon (*a*-C) film, mainly consisting of sp^2-bonded carbon atoms and sp^3-bonded carbon atoms. It often contains hydrogen atoms, whose fraction depends on the methods used to fabricate the films. DLC films are usually fabricated using physical vapor deposition methods such as the ionization-assisted deposition method or the sputtering method and chemical vapor deposition (CVD) methods such as radio-frequency plasma CVD. The properties of films mainly depend on their atomic composition, i.e., the fractions of sp^3-bonded carbon atoms, sp^2-bonded carbon atoms, and hydrogen atoms; the atomic composition of a film can be represented in a ternary phase diagram.[1–3] The Raman spectra of DLC films suggest that the films contain cluster structures that consist of sp^2-bonded atoms.[2,4,5] Therefore, it is important to investigate DLC films at the atomic level in order to understand their properties. Atomistic simulations are considered effective to obtain information at the atomic level because they directly reveal all the atomic positions.

According to literature, three types of atomistic calculations were usually employed for *a*-C: the first-principles calculations based on plane-wave density functional theory (DFT), the *ab initio* tight-binding (TB) method, and classical molecular dynamics (CMD) calculations. These calculation methods were evaluated against experiments. To evaluate a particular calculation method, the fractions of fourfold coordinated carbon atoms were calculated as a function of density by using the method, and these fractions were compared with the experimentally determined fractions of sp^3-bonded carbon atoms as a function of density. In addition, radial distribution functions (RDFs) were often used for comparisons. It is known that the fractions of fourfold coordinated carbon atoms obtained form DFT calculations[6–9] and the nonorthogonal TB method[10–13] agree with the fractions obtained from experiments, while the orthogonal TB[14,15] method underestimates these fractions. On the other hand, the fractions obtained from CMD calculations strongly depend on the interatomic potential employed in the calculations. Most of the CMD calculations were performed by employing empirical bond-order-type interatomic potentials (EBOPs):[16] the Tersoff interatomic potential for carbon proposed by Tersoff,[17] the Tersoff interatomic potential for carbon developed by Brenner,[18,19] the Tersoff interatomic potential for carbon proposed by Erhart *et al.*,[20] the Brenner interatomic potential for carbon and hydrocarbons,[21–27] reactive empirical bond order (REBO) potential,[28,29] and adaptive intermolecular REBO (AIREBO) potential.[30–32] Brenner-type interatomic potentials (i.e., Brenner potential, REBO potential, and AIREBO potential) are thought to be suitable for carbon systems since they contain correction terms, which were incorporated in order to correct an overbinding and to describe the nonlocal conjugation effects, which had not been taken into consideration in simple EBOPs such as the Abell–Tersoff potential. However, it should be noted that the fractions of fourfold coordinated carbon atoms obtained using EBOPs are remarkably underestimated[12,19,22,31] in comparison with the fractions obtained from experiments, and that the RDFs exhibit strange sharp peaks, which arise due to the cutoff functions, around the cutoff distance.[12] Another approach to obtain fractions of fourfold coordinated carbon atoms is to perform a CMD calculation using environment dependent interatomic potential (EDIP),[33,34,12,35,36] which can be classified as a cluster-type interatomic potential. It should be noted that the fractions of fourfold coordinated carbon atoms obtained using EDIP are similar to those obtained from DFT calculations to some extent; however, they are 20% lower than the fractions obtained from DFT calculations for *a*-C structures of density of 3.2 g/cm^3. Further, RDFs obtained using EDIP are similar to those determined from DFT calculations.

[a]Electronic mail: kumagai.tomohisa@fml.t.u-tokyo.ac.jp.

As a rule, the number of atoms in DFT and TB calculations performed using conventional computer systems is limited to several hundreds. The system sizes in DFT and TB calculations are adequate for most of the situations where short-range ordering and bond arrangement are important. On the other hand, CMD calculations are performed for large-scale and long-time calculations because CMD calculations for more than a thousand atoms can be performed within nanoseconds. However, CMD calculations are not suitable for quantitatively predicting the behavior of materials since the interatomic interactions are determined empirically. Therefore, improvements in the empirically determined interatomic potentials seem to contribute very little to the physical insights obtained from CMD calculations. However, the development of a suitable empirical interatomic potential for *a*-C systems will contribute to improve the accuracy of CMD calculations performed for these systems for the following two reasons: (1) *a*-C structures obtained by using normal EBOPs are significantly different from those obtained from first-principle calculations, as described above, and (2) for amorphous systems, it is known that long-time relaxation lasting several nanoseconds has an important role for reproducing experimentally obtained amorphous structures.[37] Therefore, in this study, we develop an EBOP that can reproduce the material properties of *a*-C systems.

II. DEVELOPMENT OF INTERATOMIC POTENTIALS

A. Potential function form

One of the reasons why an EBOP tends to underestimate the fractions of sp^3-bonded atoms is the short cutoff distance employed in the distance-dependent cutoff functions. Jäger *et al.* improved the applicability of the Brenner interatomic potential to *a*-C structures by increasing the cutoff distance.[22] However, a cutoff function causes strange sharp peaks in the calculated RDFs around the cutoff distance. Therefore, in order to increase the cutoff distance without causing any artificial effects, a screening function[38–40] is introduced in this research, instead of a cutoff function. If there are no screening atoms between two atoms, the value of the screening function between the two atoms is 1. This value decreases to zero as screening atoms enter the space between the two atoms deeply. The behavior of the screening function is similar to that of a cutoff function, and hence, it can be used in place of a cutoff function. It should be noted that the screening function does not lead to artificial effects. Further, the Brenner potential[21] is employed in this study as a basic potential function since many results for *a*-C systems were hitherto obtained by using this potential,[22–27] while the fractions of fourfold coordinated atoms were somewhat underestimated.

Initially, the correction terms F and H were introduced in the case of the Brenner potential[21] in order to reproduce the cohesive energies of hydrocarbons and vacancy formation energies in graphene and diamond. Cohesive energies can be reproduced by adjusting the modulus of the bonding term. The modulus of the bonding term can be varied by adding F and H to the bond order term. The values of $F(N_{ij}^t, N_{ji}^t, N_{ij}^{\mathrm{conj}})$, which is a correction term for the bond between the ith and the jth atoms, were provided at discrete points, and the values at intermediate points were obtained by tricubic spline interpolation. Here, N_{ij}^t was calculated as a coordination number of the ith atom, except for the bond between the ith and jth atoms, and N_{ij}^{conj} was a flag for determining whether a bond between the ith and jth atoms was a part of conjugated systems or not. The other correction term H, which was introduced in order to reproduce the cohesive energies of hydrocarbons, depended on both the number of bonds on carbon atoms and those on hydrogen atoms. However, H is not used in this study since hydrogen atoms are not considered.

In this study, we first remove the original corrections because the essential corrections for *a*-C systems can only be made effective once the original corrections are removed. Corrections are essential for describing the bonds between atoms that have different coordination numbers in *a*-C structures, since the values of potential parameters in EBOPs are usually determined without considering them. Correction is particularly required for the bond between a threefold coordinated atom and a fourfold coordinated atom, since *a*-C structures mainly consist of these two types of atoms. Therefore, $F(2,3,\geqslant 1)$ and $F(3,2,\geqslant 1)$ are used for the bonds, since the first two arguments of F correspond to values that are 1 smaller than the coordination numbers [i.e., the coordination numbers are 3 and 4 in $F(2,3,\geqslant 1)$ or $F(3,2,\geqslant 1)$]. These corrections were originally introduced in the Brenner potential as corrections for vacancies in diamond. As explained by Brenner, the intermediate bonding situation cannot be expressed easily without correction such as these for bonds between a threefold coordinated atom and a fourfold coordinated atom.[21] In addition, $F(1,1,\geqslant 2)$ is employed as a correction for sp-bonded carbon atoms.

A term that represents the dihedral angle potential is also added since it has been revealed that the dihedral angle effect around the bonds between sp^2-bonded carbon atoms plays an important role in liquid carbon (*l*-C) systems[41] and *a*-C systems.[19,34,36] The total energy Φ is the sum of the bond-order-type interatomic potential E^{bop} and the dihedral angle potential E^{dih}, that is,

$$\Phi = E^{\mathrm{bop}} + E^{\mathrm{dih}}. \tag{1}$$

Even if there are no screening atoms between two atoms, the atom interaction will be weak when their bonds are saturated. Therefore, the effect of bond saturation must also be considered when screening functions are introduced. In order to incorporate this saturation effect, a bond-order term is incorporated into the repulsive term, and the saturation effect in the bond-order term of the attractive term is made effective [in the original potential, the saturation effect is ineffective, i.e., $\alpha=0$ in Eq. (11)]. E^{bop} is defined as follows:

$$E^{\mathrm{bop}} = \frac{1}{2}\sum_{i\neq j} \phi_{ij}(r_{ij}), \tag{2}$$

$$\phi_{ij}(r) = f_{ij}^{\mathrm{sc}}[A\bar{a}_{ij}\exp(-\lambda_1 r) - B\bar{b}_{ij}\exp(-\lambda_2 r)], \tag{3}$$

$$A = \frac{D}{S-1}\exp(RT\sqrt{2S}), \quad B = \frac{DS}{S-1}\exp(RT\sqrt{2/S}), \tag{4}$$

$$\lambda_1 = T\sqrt{2S}, \quad \lambda_2 = T\sqrt{2/S}, \tag{5}$$

$$\bar{a}_{ij} = \frac{a_{ij} + a_{ji}}{2}, \tag{6}$$

$$a_{ij} = [1 + \zeta_{1,ij}^{\eta_1}]^{-\delta_1}, \tag{7}$$

$$\zeta_{1,ij} = \sum_{k(\neq i,j)} f_{ik}^{\mathrm{sc}} a \exp[\alpha(r_{ij} - r_{ik})^{\beta}], \tag{8}$$

$$\bar{b}_{ij} = \frac{b_{ij} + b_{ji} + F(N_{ij}^t, N_{ji}^t, N_{ij}^{\mathrm{conj}})}{2}, \tag{9}$$

$$b_{ij} = [1 + \zeta_{2,ij}^{\eta_2}]^{-\delta_2}, \tag{10}$$

$$\zeta_{2,ij} = \sum_{k(\neq i,j)} f_{ik}^{\mathrm{sc}} G(\theta) a \exp[\{\alpha(r_{ij} - r_{ik})\}^{\beta}], \tag{11}$$

$$G(\theta) = 1 + \frac{c^2}{d^2} - \frac{c^2}{d^2 + (1 + \cos\theta)^2}, \tag{12}$$

$$N_{ij}^t = \sum_{k(\neq i,j)} f_{ik}^{\mathrm{sc}}, \tag{13}$$

$$N_{ij}^{\mathrm{conj}} = 1 + \sum_{k(\neq i,j)} f_{ki}^{\mathrm{sc}} P(N_{ki}^t) + \sum_{l(\neq i,j)} f_{lj}^{\mathrm{sc}} P(N_{lj}^t), \tag{14}$$

$$P(x) = \begin{cases} 1, & x \leqslant 2 \\ \dfrac{1 + \cos[\pi(x-2)]}{2}, & 2 < x < 3 \\ 0, & x \geqslant 3, \end{cases} \tag{15}$$

where, i, j, k, and l are atomic indexes in calculation systems, r_{ij} denotes the interatomic distance between the ith and jth atoms, θ_{ijk} denotes the bond angle between the i-j bond and the i-k bond, and ω_{kijl} denotes the dihedral angle between two planes—a plane that contains the ith, jth, and kth atoms and a plane that contains the ith, jth, and lth atoms.

D, S, T, R, η_2, δ_2, a, c, and, d are the potential parameters used in the Brenner potential.[21] The values of F are provided at discrete points and are interpolated by using a tricubic spline function. α and β are potential parameters common to both bond-order terms (i.e., a_{ij} and b_{ij}) and the term that represents the effect of bond saturation (i.e., f_{ij}^{sc}). δ_1 and η_1 are the potential parameters for an added bond-order term in the repulsive term.

The dihedral angle potential is expressed as a sum of cosine functions.[42] In order to restrict the dihedral angle potential to only sp^2-bonds, its coordination dependence is introduced as follows:

$$E^{\mathrm{dih}} = \frac{1}{2}\sum_i \sum_{j(\neq i)} \sum_{k(\neq i,j)} \sum_{l(\neq i,j,k)} f_{ki}^{\mathrm{sc}} f_{ij}^{\mathrm{sc}} f_{jl}^{\mathrm{sc}} f_{ij}^{\mathrm{dih}}(\omega_{kijl}), \tag{16}$$

$$V_{ij}^{\mathrm{dih}}(\omega) = \sum_{k=1}^{6} C_k^{\mathrm{dih}}(N_i, N_j)\{1 - (-1)^k \cos(k\omega)\}, \tag{17}$$

$$N_i = \sum_{j(\neq i)} f_{ij}^{\mathrm{sc}}, \tag{18}$$

where $C_k^{\mathrm{dih}}(N_i, N_j)$ depends on the coordination numbers of the atoms that form a bond as the axis of rotation in the dihedral angle (i.e., the ith and jth atoms in the k-i-j-l atoms). The values of C_k^{dih} are given at discrete points and are interpolated at intermediate points by using a bicubic spline function.

f_{ij}^{sc} is a screening function between the ith and jth atoms, proposed by Baskes,[40] as follows; it is given

$$f_{ij}^{\mathrm{sc}} = \prod_{k(\neq i,j)} S_{ijk}, \tag{19}$$

$$S_{ijk} = f_c\left[\frac{C_{ijk} - C_{\min}}{C_{\max} - C_{\min}}\right], \tag{20}$$

$$C_{ijk} = \frac{2(X_{ik} + X_{jk}) - (X_{ik} - X_{jk})^2 - 1}{1 - (X_{ik} - X_{jk})^2}, \tag{21}$$

$$X_{ik} = \left(\frac{r_{ik}}{r_{ij}}\right)^2, \quad X_{jk} = \left(\frac{r_{jk}}{r_{ij}}\right)^2, \tag{22}$$

$$f_c(x) = \begin{cases} 1, & x \geqslant 1 \\ [1 - (1-x)^4]^2, & 0 < x < 1 \\ 0, & x \leqslant 0. \end{cases} \tag{23}$$

B. Potential parameters

For the Brenner potential functions, two potential parameter sets, which were set I and set II, were developed.[21] Set I was developed mainly to reproduce the atomic structures of carbon and set II was developed mainly to reproduce the elastic properties of carbon. In this study, most of the values in set I are used since the objective of this study is to reproduce the atomic structures of a-C. For example, it was possible to reproduce the fractions of fourfold coordinated atoms in a-C structures by using the increased cutoff distance proposed by Jäger *et al.* along with set I.[22]

In order to reproduce the interatomic interactions around equilibrium states, various material properties of equilibrium crystals, namely, graphite and diamond crystals, are used for fitting since most of local a-C structures are around equilibrium states. In order for a threefold coordinated atom and a fourfold coordinated atom to be stable in a-C systems, cohesive energies of various carbon polytypes are also used for fitting. The bond energies and the equilibrium bond lengths of bonds between threefold coordinated atoms and those of bonds between fourfold coordinated atoms, which were calculated using the Brenner (I) potential, agreed with the experimentally obtained values for sp^2 and sp^3 bonds, respectively, while the spring constants which were calculated by using the Brenner (I) potential were underestimated. Therefore, the parameters of the Brenner (I) potential, which

TABLE I. Meterial properties of diamond obtained using the developed potential. In this table, E_c, a, and C_{ij} represent the cohesive energy, lattice constant, and elastic constants, respectively. E_f^v, $E_f^{I_T}$, $E_f^{I_S}$, and $E_f^{I_B}$ represent defect formation energies for single vacancy, tetragonal interstitial, ⟨100⟩ split interstitial, and bond centered interstitial, respectively.

	This study	Brenner (I)[a]	Expt.[b] (DFT[c])
E_c (eV/atom)	7.3464	7.3464	7.342
a (Å)	3.558	3.558	3.567
C_{11} (GPa)	350	350	1076
C_{12} (GPa)	197	197	125
C_{44} (GPa)	277	277	576
E_f^v (eV)	1.7	7.1	(7.2)
$E_f^{I_T}$ (eV)	7.1	7.3	(23.6)
$E_f^{I_S}$ (eV)	5.1	3.7	(16.7)
$E_f^{I_B}$ (eV)	4.8	7.7	(15.8)

[a]All Brenner (I) data are recalculated.
[b]From Ref. 53.
[c]From Ref. 54.

TABLE II. Material properties of graphite obtained using the developed potential. In this table, the symbols are identical to those in Table I, and $E_f^{I_H}$ represents defect formation energy for hexagonal interstitial. The elastic constants are those of graphites that have the experimental c/a ratio [i.e., 1.364 (Ref. 53)].

	This study	Brenner (I)[a]	Expt. (DFT[b])
E_c (eV/atom)	7.3767	7.3767	7.381[c]
a (Å)	2.459	2.459	2.459[c]
C_{11} (GPa)	557	557	1060[d]
C_{12} (GPa)	54	54	180[d]
C_{66} (GPa)	251	251	440[d]
E_f^v (eV)	6.7	7.5	(7.6)
$E_f^{I_H}$ (eV)	14.7	15.0	(9.2)
$E_f^{I_B}$ (eV)	4.6	5.6	(19.5)

[a]All Brenner (I) data are recalculated.
[b]From Ref. 55.
[c]From Ref. 53.
[d]From Ref. 56.

mainly describe the material properties of carbon crystals, are used so that the material properties of carbon crystals which are obtained by using the Brenner (I) potential remain unchanged.

The values of the other potential parameters are adjusted so that the material properties of a-C structures, such as the fractions of fourfold coordinated atoms and RDFs, can be reproduced. The methods used to determine the values of the potential parameters are detailed in Appendix; the values of the parameters that were determined are also given in Appendix. It should be noted that the values of $F(2,3,\geqslant 1)$, $F(3,2,\geqslant 1)$, which work for the corrections for the bonds between a threefold coordinated atom and a fourfold coordinated atom, are negative. That is, the bonds between a threefold coordinated atom and a fourfold coordinated atom are weakened owing to the correction term F.

III. RESULTS

In order to investigate the effects of the improvements, the basic material properties of carbon are derived. The material properties of diamond and graphite obtained by using the developed potential are shown in Tables I and II, respectively. These results agree well with those obtained using the Brenner (I) potential, except in the case of defect formation energies. Further, these defect formation energies are different from those obtained from first-principles calculations. Most of the defect formation energies have been underestimated. The underestimation of the vacancy formation energy in diamond is especially serious. The estimated elastic constants are also lower than those obtained from experiments. However, the underestimation of elastic constants cannot be avoided since it is the shortcomings of the Brenner (I) potential.

The underestimated defect formation energies and elastic constants may have some effect on the CMD calculations for a-C systems, when the developed potential is employed. The effects of the underestimations on nonequilibrium a-C systems may not be small since many defects are formed and local pressure is applied in nonequilibrium states. However, the developed potential can be applied to most equilibrium a-C structures since the effects of underestimations are limited in this case. This is because most of the defects vanish during the local structural relaxation of a-C in models of equilibrium a-C structures; further, the effects of elastic properties on equilibrium states are small. Very few defects were present in the a-C structures obtained from CMD calculations by using the developed potential, even though most defect formation energies were underestimated. The experimentally obtained dangling-bond densities of a-C were also very low [e.g., $10^{17}-10^{20}/\mathrm{cm}^3$ (Ref. 1)] relative to the system size considered in molecular simulations.

It is natural that the material properties of carbon crystals obtained by using the developed potential are not improved from those obtained by using the Brenner (I) potential since the improvements have been incorporated into the Brenner potential (I) to ensure that the material properties of carbon crystals remain unchanged. If an EBOP that reproduces the material properties of carbon crystals is required, it can be obtained by applying the improvements used in this study (i.e., the use of the screening function and the development of the dihedral angle potential) to an EBOP that accurately reproduces the experimentally observed material properties of carbon crystals. For example, when the improvements were made to the Brenner (II) potential, we obtained an EBOP that could reproduce the elastic properties of graphite and diamond.

The relative energies of carbon polytypes calculated using the developed potential are similar to those obtained by using the Brenner (I) potential, as shown in Table III. The equilibrium bond lengths of carbon polytypes calculated using the developed potential are also similar to or better than those obtained by using the Brenner (I) potential, as shown in Table IV.

In order to evaluate the applicability of the developed potential to a-C systems, a-C structures are modeled using liquid quench methods. In this study, the densities are set to 2.0, 2.3, 2.6, 2.9, and 3.2 $\mathrm{g/cm}^3$. The initial structures consist of 1000 carbon atoms placed randomly. The structures are heated to 8000 K, maintained at 8000 K for 1.4 ps, and

TABLE III. Relative cohesive energies of carbon polytypes calculated using the developed potential and the Brenner (I) potential.

	Relative cohesive energy (eV/atom)		
	This study	Brenner (I)	Expt.[a] (DFT)
Dimer	4.184	4.184	4.238
Chain	0.838	1.169	(0.841[c])
Graphite	−0.030	−0.030	−0.020
Diamond	0.000	0.000	0.000
SC	1.893	1.891	(2.66,[b] 2.622[c])
bcc	3.699	2.628	(4.28,[b] 4.218[c])
fcc	4.663	3.214	(4.59,[b] 4.429[c])

[a]From Ref. 53.
[b]From Ref. 57.
[c]Calculated using VASP (Refs. 44 and 45).

then quenched from 8000 to 0 K at the rate of 2 K/fs in an *NVT* ensemble. The cutoff distances are chosen on the basis of the density: 4.3 Å for 2.0 g/cm^3, 4.2 Å for 2.3 g/cm^3, 4.1 Å for 2.6 g/cm^3, 4.0 Å for 2.9 g/cm^3, and 3.9 Å for 3.2 g/cm^3. In order to improve the accuracy of the calculations, the results of CMD calculations are averaged over 12 cases. The material properties of *a*-C structures, except for the ring statistics, are calculated by being averaged during annealing for 1.0 ps at 273 K. The ring statistics are calculated on the basis of the shortest path ring[43] only when the final structures are obtained after annealing because the calculation of ring statistics is an expensive process. It is acceptable because the calculation of the ring statistics at snapshot is acceptable since ring statistics remained almost unchanged during the annealing.

The fractions of fourfold coordinated atoms and threefold coordinated atoms are shown in Figs. 1 and 2, respectively. These fractions agree with those obtained from the DFT calculations. The fractions of fourfold coordinated atoms also agree with the fractions of sp^3-bonded atoms obtained from experiments.

RDFs of *a*-C structures with the densities of 2.0, 2.6, 2.9, and 3.2 g/cm^3 obtained using the developed potential are shown in Fig. 3. The profiles of RDFs are similar to those obtained from DFT calculations for all densities. To some extent, the RDF of the *a*-C structure with a density of 3.2 g/cm^3 has a profile similar to that from the experiments.

TABLE IV. Equilibrium bond lengths of carbon polytypes calculated using the developed potential and the Brenner (I) potential.

	Equilibrium bond length (Å)		
	This work	Brenner (I)	Expt.[a] (DFT)
Dimer	1.315	1.315	1.2425
Chain	1.303	1.325	(1.275[a])
Graphite	1.419	1.419	1.420
Diamond	1.541	1.541	1.545 (1.537,[b] 1.547[c])
SC	1.833	1.767	(1.770,[b] 1.774[c])
bcc	2.144	1.826	(2.057,[b] 2.055[c])
fcc	2.415	1.872	(2.176,[b] 2.179[c])

[a]From Ref. 53.
[b]From Ref. 57.
[c]Calculated using VASP (Ref. 44 and 45).

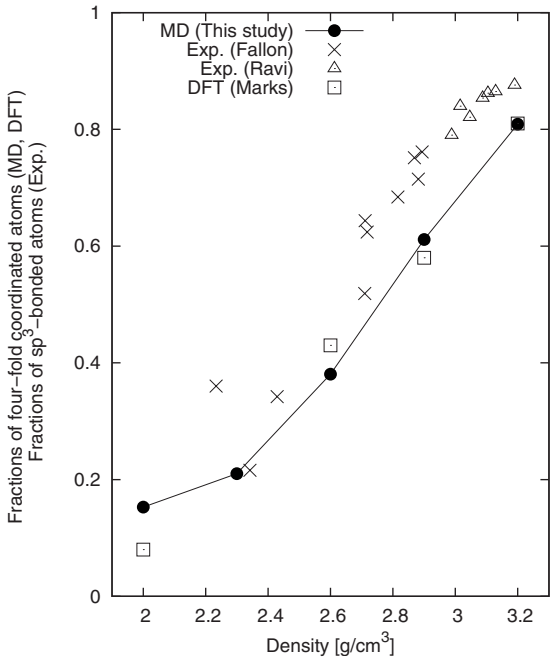

FIG. 1. Fractions of fourfold coordinated carbon atoms in *a*-C structures obtained from the developed potential. The coordination number is calculated by counting the bonds for which (1) the values of the cutoff functions are greater than 0.5 and (2) the lengths are less than 1.85 Å. Experimental data indicated by Exp. (Fallon) and Exp. (Ravi) are taken from Refs. 50 and 51, respectively. DFT data are taken from Ref. 12.

No artificial peaks are observed in these RDFs. However, such peaks were observed in RDFs of *a*-C structures obtained by using the Brenner potential owing to the cutoff function.[12]

The ring statistics obtained using the developed potential are shown in Fig. 4. The statistics agree with those obtained from the DFT calculations of *a*-C structures of densities of

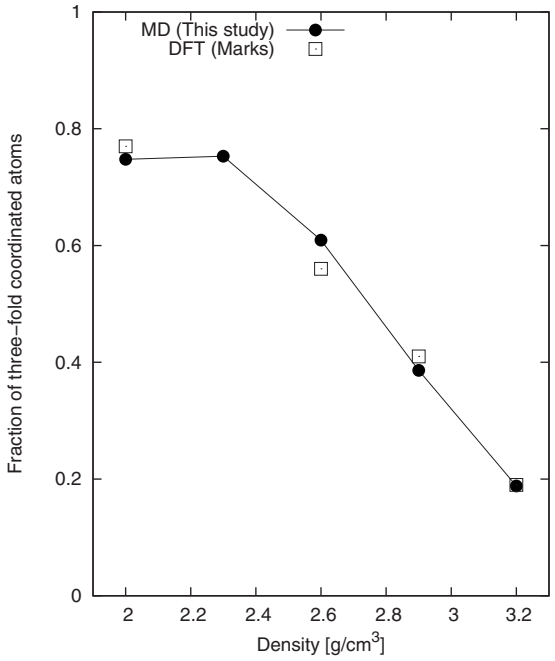

FIG. 2. Fractions of threefold coordinated carbon atoms in *a*-C structures obtained using the developed potential. DFT data are taken from Ref. 12.

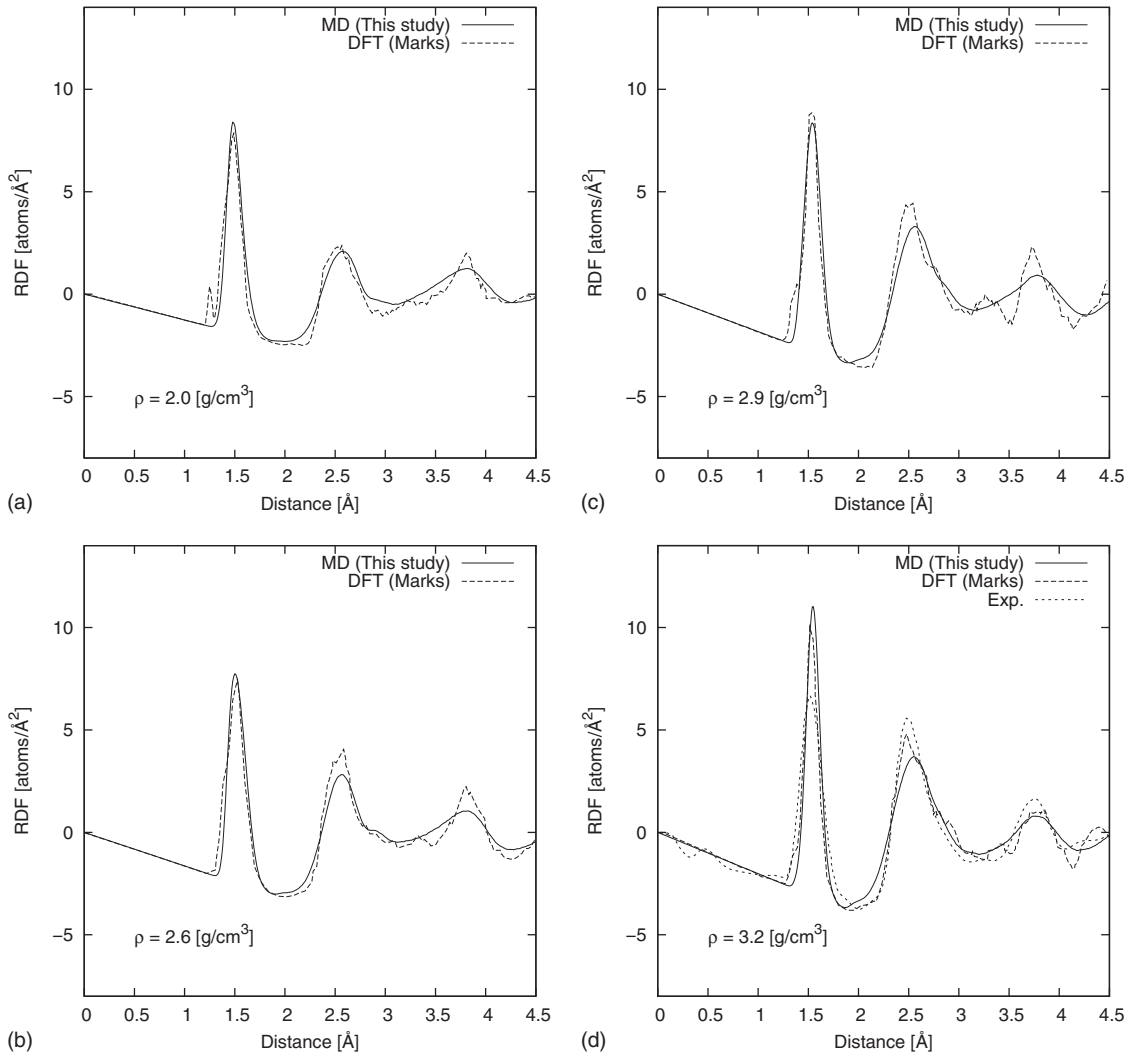

FIG. 3. RDFs of *a*-C structures obtained using the developed potential. DFT data are taken from Ref. 12. Experimental data is taken from Ref. 52.

2.6, 2.9, and 3.2 g/cm^3. However, our results appear to be different from those obtained from the DFT calculation for a density of 2.0 g/cm^3. This discrepancy is due to the difference in the calculation conditions between the two methods. In the DFT calculation, the number of atoms in the supercell at 2.0 g/cm^3 was only 125. When *a*-C structures with density of 2.0 g/cm^3 which contain 125 atoms were calculated by using the developed potential, we found similar ring statistics of *a*-C structures among them to that obtained from the DFT calculation.

The clear peak is observed for a five-membered ring in the ring statistics of *a*-C with a density of 2.0 g/cm^3; it is also observed for a six-membered ring in the ring statistics of *a*-C with a density of 2.3 g/cm^3, which is not shown in Fig. 4. The peaks correspond to a plane five-membered ring and a plane six-membered ring, which are formed due to the dihedral angle potential.

IV. DISCUSSION

The correction term F, which includes the repulsive force for the bonds between a threefold coordinated atom and a fourfold coordinated atom, may cause bond formation between threefold coordinated atoms and between fourfold coordinated atoms. To confirm this, T, T^4, T_4, and T_4^4 are introduced. T is defined as the sum of the coordination numbers of all atoms in a primary cell. T^4 is defined as the sum of the coordination numbers of fourfold coordinated atoms in a primary cell. T_4 is defined as the sum of the number of fourfold coordinated atoms that connect to the ith atom N_i^4 with respect to all atoms; that is, it is $\Sigma_i^n N_i^4$, where n is the number of atoms in a primary cell. T_4^4 is defined as the number of fourfold coordinated atoms that connect to the ith atom N_i^4 with respect to fourfold coordinated atoms; it is $\Sigma_i^{n_4} N_i^4$, where n_4 is the number of fourfold coordinated atoms in the primary cell. T equals twice the total number of bonds, since the bond between the ith and jth atoms is counted twice; that is, the coordination numbers of both the ith and jth atoms are counted. It should be noted that T^4 is equal to T_4, that $T^4(=T_4)$ is equal to four times the number of fourfold coordinated atoms, and that T_4^4 is equal to twice the number of bonds between fourfold coordinated atoms. Schematic illustrations of the counting methods for T, T^4, T_4, and T_4^4 are shown in Fig. 5.

The ratio T_4^4/T^4 is considered to be the probability that the end of a bond from a fourfold coordinated atom is connected to a fourfold coordinated atom. The ratio T_4/T is

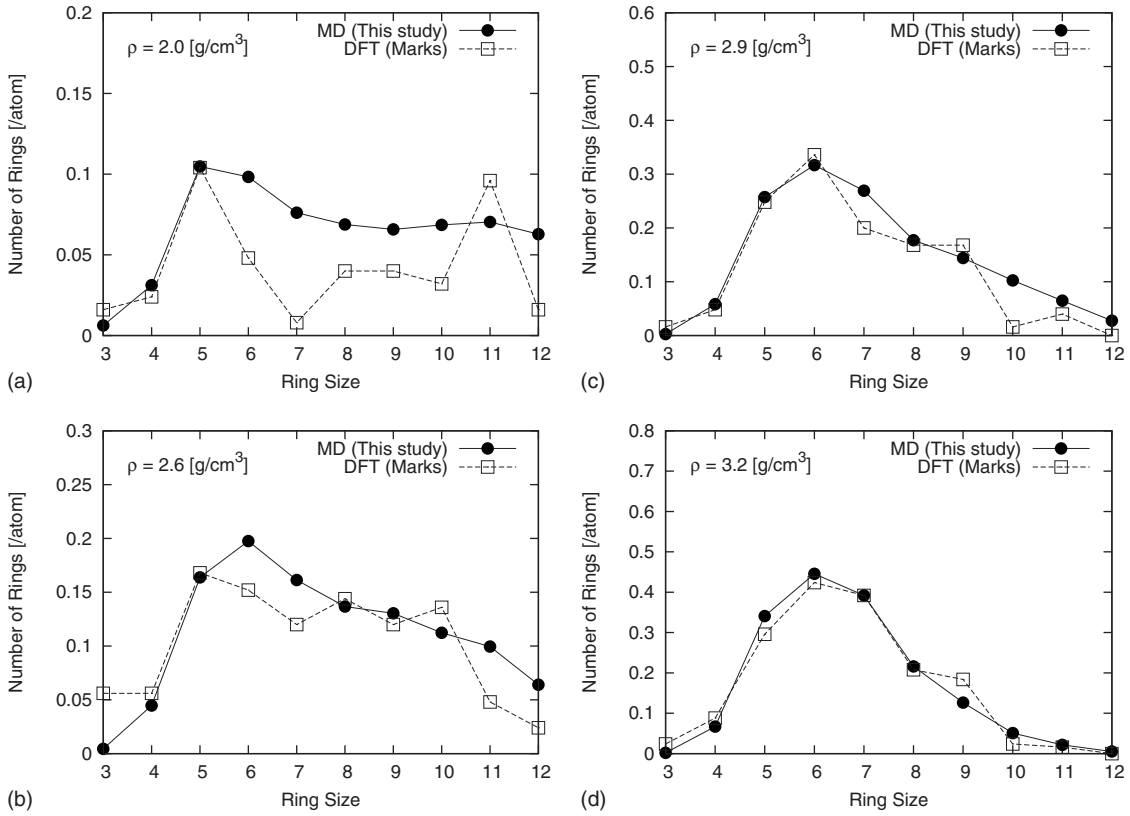

FIG. 4. Ring statistics of amorphous carbon structures obtained using the developed potential. DFT data are taken from Ref. 12.

considered to be the averaged probability that the end of a bond is connected to a fourfold coordinated atom. The relative formation ratio of the bonds between fourfold coordinated atoms can be evaluated by comparing T_4/T with T_4^4/T^4. These ratios obtained using Pot. II, III, IV, and V are shown and compared with those obtained from DFT calculations shown in Table V. The ratio $T \cdot T_4^4/T^4 \cdot T_4$ corresponds to the ratio of formation of bonds between fourfold coordinated atoms whose reference value is 1.

In this study, DFT calculations are performed by employing VASP,[44,45] which is a commercial plane-wave density functional code. In the DFT calculations, a supercell contains 160 carbon atoms. *a*-C structures are modeled using the liquid-quenching method at the rate of 2 K/fs from 6000 to 0 K. Non-spin-polarized generalized gradient approximation (GGA) proposed by Perdew and Wang is employed for the exchange-correlation functional.[46] Ion-valence electron interactions are represented by an ultrasoft pseudopotential. Only the gamma point is used for Brillouin-zone sampling with an energy cutoff of 287 eV.

It is confirmed that T_4^4/T^4 is always larger than T_4/T in *a*-C structures obtained using the developed potential for each density. This trend is also confirmed for the *a*-C structures obtained from DFT calculations. The results suggest the formation of cluster structures that mainly consist of bonds between fourfold coordinated atoms. When we employ EBOPs which do not contain the repulsive correction for the bonds between a threefold coordinated atom and a fourfold coordinated atom, threefold coordinated atoms and fourfold coordinated atoms are mixed and the cluster structures are not confirmed.

V. SUMMARY

In this study, an empirical bond-order-type interatomic potential that can reproduce carbon crystals and *a*-C struc-

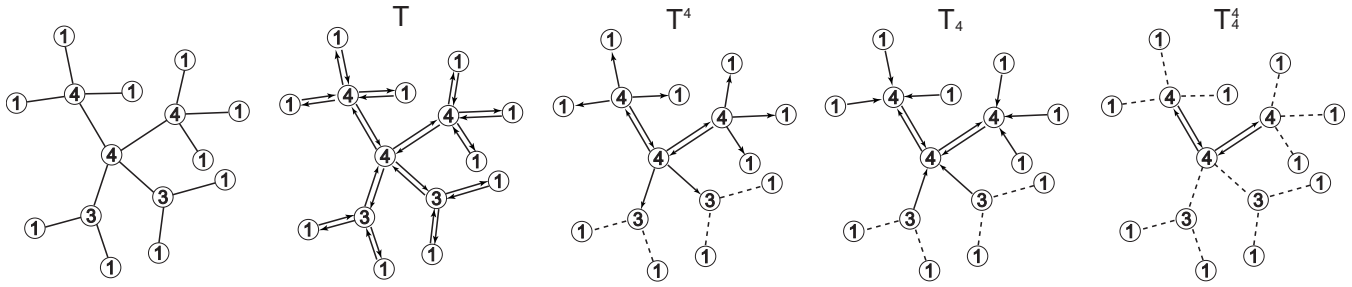

FIG. 5. Schematic illustrations of counting methods for T, T^4, T_4, and T_4^4. A circle and the inscribed number represent an atom and its coordination number, respectively.

TABLE V. Fractions of fourfold coordinated atoms around fourfold coordinated atoms T_4^4/T^4 as compared to averaged fractions of fourfold coordinated atoms around all atoms T_4/T for a-C structures obtained using the developed potential. DFT data also shown for comparison.

	This study			DFT[a]		
ρ (g/cm^3)	$\frac{T_4^4}{T^4}$	$\frac{T_4}{T}$	Ratio	$\frac{T_4^4}{T^4}$	$\frac{T_4}{T}$	Ratio
2.0	0.33	0.20	1.63	0.33	0.16	2.04
2.3	0.37	0.27	1.40	0.41	0.26	1.58
2.6	0.54	0.45	1.19	0.62	0.47	1.31
2.9	0.72	0.68	1.06	0.78	0.70	1.11
3.2	0.85	0.85	1.01	0.93	0.90	1.02

[a]Calculated using VASP (Refs. 44 and 45).

tures was developed by adding several improvements to the Brenner potential. By using the developed potential, the following material properties of a-C structures obtained from DFT calculations were reproduced: the fraction of fourfold coordinated atoms as a function of a-C density, the RDFs, and ring statistics. The material properties of carbon crystals obtained using the developed potential are similar to or improved from those by obtained using the Brenner (I) potential except for defect formation energies. A screening function is employed instead of a cutoff function. The effect of bond saturation is incorporated as a bond-order term in the repulsive term. A dihedral angle potential for the rotation around a bond between threefold coordinated atoms is introduced. The values of potential parameters of the Brenner (I) potential are used for potential parameters that determine the material properties of crystals. The values of the other potential parameters (i.e., those in added terms in this study, a correction term, and terms that represent bond saturation effects in bond-order terms) are adjusted to reproduce a-C structures under the condition that their effects on the carbon crystals are as small as possible. It is found that the correction term enhances the formation of cluster structures in a-C, which is also observed in the first-principles calculation.

ACKNOWLEDGMENTS

The authors wish to express their sincere gratitude to Professor S. Maruyama for his advice in developing the program on the Brenner potential and for insightful suggestions for developing the dihedral angle potential. We specially thank to Professor Y. Shibuta who offered us an excellent computer environments. This study was supported by a Grant-in-Aid for Young Scientists (B) No. 20760065 from MEXT.

APPENDIX: POTENTIAL PARAMETER DETERMINATION

In this section, we describe the methods used to determine the values of potential parameters. In order to avoid changes in the material properties of carbon crystals obtained using the original Brenner potential, the values of the original Brenner potential parameter set I are used for the potential parameters that determine the material properties of carbon crystals. These parameters are D, S, R, a, c, d, η_2, and δ_2. The values of the other potential parameters are adjusted so that the material properties of a-C structures are reproduced under the condition that their effects on the material properties of carbon crystals are as small as possible. These parameters are α, β, η_1, δ_1, C_k^{dih}, F, $C_{\max}$, and $C_{\min}$.

The effects of α and β on the material properties of carbon crystals are small, since same bond lengths can be assumed (i.e., $r_{ij}-r_{ik}=0$) in most crystals. In order to ensure that the values of $C_k^{\mathrm{dih}}(N_i,N_j)$ are effective only for bonds between sp^2-bonded atoms, all values of $C_k^{\mathrm{dih}}(N_i,N_j)$, except for $C_k^{\mathrm{dih}}(3,3)$, are set to zero. Further, in order to prevent changes in the material properties of carbon crystals obtained using the original Brenner potential, the values of a_{ij} are kept as 1 for any local atomic environment in carbon crystals, since these values can be considered as 1 in the original Brenner potential. Therefore, in Eq. (7), we determined the value of η_1 so that the value of a_{ij} is almost 1 for $\zeta_{1,ij}\leqslant 11$, since the value of $1+\zeta_{1,ij}$ is 12, even in the closest packed crystals. (It should be noted that the value of $1+\zeta_{1,ij}$ is considered to be the coordination number.) In order to ensure consistency between the bond-order terms in the repulsive term and the attractive term, the value of δ_1 is determined so that $\eta_1\times\delta_1$ is equal to $\eta_2\times\delta_2$.

In the case of most crystals, the values of the screening function employed for the first neighbor atoms are usually 1, and those for the second neighbor atoms are usually zero, when the general values of the parameters are selected (i.e., $C_{\max}=2.8$ and $C_{\min}=0.8-2.0$).[38–40] In such cases, the effects of the values of the screening function on the material properties of carbon crystals whose equilibrium bond lengths are lesser than R_1 in the cutoff function (i.e., 1.7 Å) are very small. Therefore, the value of $C_{\max}$ is determined to be 2.8, which is a general value for this cutoff function,[38–40] and that of $C_{\min}$ is adjusted in the range of 0.8–2.0.

$F(1,1,\geqslant 2)$, which is the only exception, is used for correcting the material properties of a crystal. The value of $F(1,1,\geqslant 2)$ is determined so that the cohesive energy of a carbon straight chain obtained from DFT calculations is reproduced. DFT calculations are performed by using VASP.[44,45] The atomic positions are optimized by using the conjugate gradient (CG) method. Two carbon atoms are present in the supercell. The spin-polarized GGA proposed by Perdew *et al.*[47] is employed as an exchange-correlation functional. The projector augmented wave (PAW) method,[48] in the implementation by Kresse and Joubert,[49] is used to describe the electron-ion interaction. The energy cutoff of the plane-wave basis is set to 900 eV.

The value of $C_k^{\mathrm{dih}}(3,3)$ is determined such that the dihedral angle potentials reproduce the conformation energy around a bond between threefold coordinated atoms determined from several first-principles calculations. It should be noted that there is no effect of the dihedral angle potential on the cohesive energy and lattice constant of graphene, since the value is set to zero for an ideal graphene structure. Because it is difficult to consider pure torsion around an sp^2 bond, the dihedral angle potential is estimated from the following three atomic structures: a graphite structure, half of which is rotated through 90°, as shown in Fig. 6(a) (cross graphite), a graphene structure, in which half of the structure is waved, as shown in Fig. 6(b) (half-waved graphene), and a

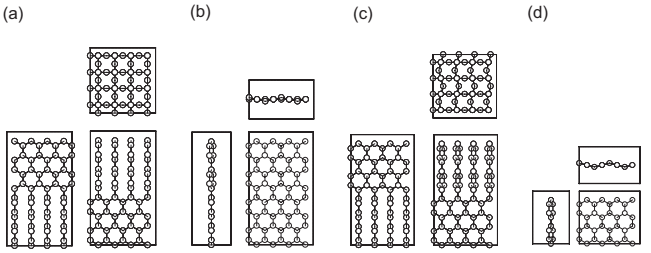

FIG. 6. Ball and stick model of atomic structures used for calculating Φ_{sp2sp2}. (a) Cross graphite ($4\times4\times1$ cells), (b) half-waved graphene ($2\times1\times1$ cells), (c) half-waved cross graphene ($4\times2\times1$ cells), and (d) waved graphene ($2\times1\times2$ cells)

graphite structure, half of which is rotated 90° and the other half of which is waved, as shown in Fig. 6(c) (half-waved cross graphite). The energies of these structures are calculated using VASP.[44,45] Atomic positions are optimized using the CG method. The GGA proposed by Perdew *et al.*[47] with spin polarization is employed for the exchange-correlation functional. The interaction between the ionic cores and valence electrons is described by the PAW method[48] in the implementation of Kresse and Joubert.[49] The energy cutoff of the plane-wave basis is set to 500 eV.

Because cross graphite has two 90° dihedral angles, $\Phi^{\mathrm{Dih}}_{sp2sp2}(\pi/2)$ can be written as

$$\Phi^{\mathrm{Dih}}_{sp2sp2}\left(\frac{\pi}{2}\right)=\Phi^{\mathrm{Dih}}_{sp2sp2}(0)+\frac{E^{\mathrm{cr}}_{\mathrm{grt}}-E_{\mathrm{grt}}}{2}, \tag{A1}$$

where E_{grt} and E^{c}_{grt} represent the energies per unit cell of graphite and cross graphite, respectively. In order to impose a periodic boundary condition, which is required in the plane-wave method, the interlayer distance is set to be the same as the width of a six-member ring.

Because half-waved graphene, in which the angle between the graphene plane of the waved part and that of the unwaved part is θ (called θ half-waved graphene in this paper), has four dihedral angles having the same value θ, $\Phi^{\mathrm{Dih}}_{sp2sp2}(\theta)$ can be written as

$$\Phi^{\mathrm{Dih}}_{sp2sp2}(\theta)=\Phi^{\mathrm{Dih}}_{sp2sp2}(0)+\frac{E^{\mathrm{hw}}_{\mathrm{grp}}(\theta)-E_{\mathrm{grp}}-E^{\mathrm{w}}_{\mathrm{grp}}(\theta)}{4}, \tag{A2}$$

where E_{grp} is the energy of graphene in its primary cell, $E^{\mathrm{w}}_{\mathrm{grp}}$ is the energy of waved graphene in its primary cell, and $E^{\mathrm{hw}}_{\mathrm{grp}}(\theta)$ is the energy of θ half-waved graphene in its primary cell. In this case, the numbers of atoms in the primary cells of graphene, waved graphene, and half-waved graphene are 16, 16, and 32, respectively. However, precise estimation of the dihedral angle potential is difficult, when the strain energy is large. Therefore, we employed these structures to determine the dihedral angle potential only for small angles, which have small strain energies in half-waved graphene structures.

Because half-waved cross graphite along the z direction, in which the angle between the waved and the unwaved parts is $\pi/2-\theta$ (called θ half-waved cross graphite in this paper), has four angles whose values are $\pi/2-\theta$, $\Phi^{\mathrm{Dih}}_{sp2sp2}(\pi/2-\theta)$ can be written as

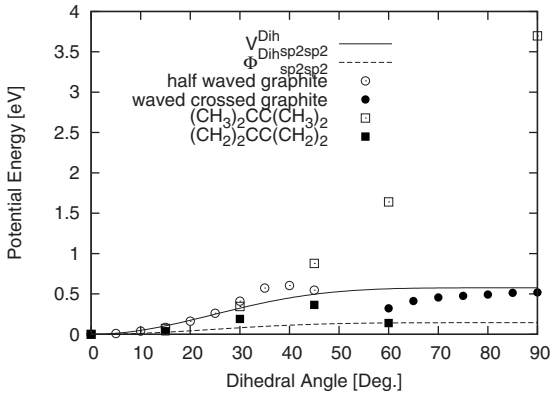

FIG. 7. $V^{\mathrm{Dih}}_{sp2sp2}(\theta)$ and $\Phi^{\mathrm{Dih}}_{sp2sp2}(\theta)$ as a function of the dihedral angle. The energies of the molecules are obtained from Ref. 41.

$$\Phi^{\mathrm{Dih}}_{sp2sp2}\left(\frac{\pi}{2}-\theta\right)=\Phi^{\mathrm{Dih}}_{sp2sp2}\left(\frac{\pi}{2}\right)+\frac{E^{\mathrm{wc}}_{\mathrm{grt}}(\theta)-E^{c}_{\mathrm{grt}}-(E^{\mathrm{w}}_{\mathrm{grt}}(\theta)-E_{\mathrm{grt}})}{4}, \tag{A3}$$

where E_{grt} is the energy of graphite in its primary cell, E^{c}_{grt} is the energy of cross graphite in its primary cell, and E^{w}_{grt} is the energy of waved graphite, which is layered waved graphene, in its primary cell, and $E^{\mathrm{wc}}_{\mathrm{grt}}(\theta)$ is the energy of θ waved cross graphite in the primary cell. In this case, the numbers of atoms in the primary cells of graphite, waved graphite, cross graphite, and waved cross graphite are 16, 16, 32, and 32, respectively. Precise estimation of the dihedral angle potential is also difficult when the strain energy is too large. Therefore, we employed these structures for the dihedral angle potential only for values of small θ, which have small strain energies in half-waved graphite structures (i.e., large dihedral angle).

By merging these results from first-principles calculations, we obtained $\Phi^{\mathrm{Dih}}_{sp2sp2}$, which is shown in Fig. 7, when $\Phi^{\mathrm{Dih}}_{sp2sp2}$ is considered to be zero. As references, the dihedral angle potentials for $(CH_3)_2CC(CH_3)_2$ and $(CH_3)_3CC(CH_3)_3$ calculated by Wu[41] are shown. Our results agree with Wu's results in the region of low dihedral angles, but not in the region of high dihedral angles. This difference is considered to arise from the difference between bulk structures and atomic clusters.

The values of $C^{\mathrm{Dih}}_{k}(3,3)$ ($k=1-6$) are determined so that the energies of these first-principles calculations are reproduced. As a result, we obtained $V^{\mathrm{Dih}}_{sp2sp2}$ as shown in Fig. 7. Calculated $\Phi^{\mathrm{Dih}}_{sp2sp2}$ from $V^{\mathrm{Dih}}_{sp2sp2}$ is also shown in Fig. 7.

The obtained values of the dihedral angle potential parameters are shown in Table VI. Note that the stacking fault energy obtained using the developed potential by employing

TABLE VI. Dihedral angle potentials. The values of the other dihedral potential parameters which are not shown in this table are zero.

k	M	N	$C^{\mathrm{dih}}_{k}(M,N)$
2	3	3	0.068 000 0
4	3	3	0.026 000 0
6	3	3	0.004 000 0

TABLE VII. Values of potential parameters determined in this research. The values of F not shown in this table are zero.

Parameters	Value	Determination method
D	6.325	Same as Brenner(I)
S	1.29	Same as Brenner(I)
R	1.315	Same as Brenner(I)
T	1.5	Same as Brenner(I)
a	0.011 304	Same as Brenner(I)
c	19	Same as Brenner(I)
d	2.5	Same as Brenner(I)
α	1.9	Adjusted for a-C
β	3	Adjusted for a-C
η_1	4	$a_{ij}=1$ when ζ_1 is small
η_2	1	Same as Brenner(I)
δ_1	0.201 173	$\eta_1\times\delta_1=\eta_2\times\delta_2$
δ_2	0.804 69	Same as Brenner(I)
$F(1,1,\geqslant 2)$	0.030 90	Adjusted for C-chain
$F(2,3,\geqslant 1)$	−0.041 85	Adjusted for a-C
$F(3,2,\geqslant 1)$	−0.041 85	Adjusted for a-C
$C_{\max}$	2.8	Same as Baskes
$C_{\min}$	1.6	Adjusted for a-C

this dihedral angle potential does not agree completely with the experimental values due to the imperfect screening effect and the inactive saturation effect in the dihedral angle potential. It should also be noted that the energy of cross graphite cannot be reproduced because the values of N_i^{dih} are 5, which include not only three in-plane atoms but also two out-of-plane atoms due to the inactive saturation effect in the dihedral angle potential (i.e., $a^{\mathrm{dih}}=0$).

$F(2,3,\geqslant 1)=F(3,2,\geqslant 1)$, $C_{\min}$, α, and β are used to reproduce the material properties of a-C structures. They are adjusted such that both the fractions of fourfold coordinated atoms and RDFs for a-C structures obtained using the developed interatomic potential agree with those obtained from DFT calculations. Many a-C structures are modeled by using various interatomic potentials that have a wide range of values of the adjusting potential parameters. Then, we select an interatomic potential so that the material properties of a-C structures are well reproduced by it. As a result, we find useful values for the potential parameters, as shown in Table VII.

[1] *Properties of Amorphous Carbon*, edited by S. R. P. Silva, (INSPEC, London, 2003).
[2] J. Robsertson, Mater. Sci. Eng. R. **129**, 37 (2002).
[3] W. Jacob and W. Möller, Appl. Phys. Lett. **63**, 1771 (1993).
[4] S. Prawer, K. W. Nugent, Y. Lifshitz, G. D. Lempert, E. Grossman, J. Kulik, I. Avigal, and R. Kalish, Diamond Relat. Mater. **5**, 433 (1996).
[5] A. C. Ferrari and J. Robertson, Phys. Rev. B **61**, 14095 (2000).
[6] G. Galli, R. M. Martin, R. Car, and M. Parrinello, Phys. Rev. B **42**, 7470 (1990).
[7] N. A. Marks, D. R. McKenzie, B. A. Pailthorpe, M. Bernasconi, and M. Parrinello, Phys. Rev. Lett. **76**, 768 (1996).
[8] D. G. McCulloch, D. R. McKenzie, and C. M. Goringe, Phys. Rev. B **61**, 2349 (2000).
[9] S. Uhlmann, Th. Frauenheim, and Y. Lifshitz, Phys. Rev. Lett. **81**, 641 (1998).
[10] Th. Frauenheim, P. Blaudeck, U. Stephan, and G. Jungnickel, Phys. Rev. B **48**, 4823 (1993).
[11] U. Stephan, Th. Frauenheim, P. Blaudeck, and G. Jungnickel, Phys. Rev. B **50**, 1489 (1994).
[12] N. A. Marks, N. C. Cooper, D. R. McKenzie, D. G. McCulloch, P. Bath, and S. P. Russo, Phys. Rev. B **65**, 075411 (2002).
[13] T. Kugimiya and Y. Shibutani, Trans. Jpn. Soc. Mech. Eng., Ser. A **67**, 632 (2001).
[14] C. Z. Wang and M. Ho, Phys. Rev. Lett. **71**, 1184 (1993).
[15] C. Z. Wang and K. M. Ho, Phys. Rev. B **50**, 12429 (1994).
[16] E. Neyts, Ph.D. thesis, University of Antwerpen, 2006.
[17] J. Tersoff, Phys. Rev. Lett. **61**, 2879 (1988).
[18] D. W. Brenner, Mater. Res. Soc. Symp. Proc. **141**, 59 (1989).
[19] T. Kugimiya and Y. Shibutani, Trans. Jpn. Soc. Mech. Eng., Ser. A **66**, 1794 (2000).
[20] P. Erhart and K. Albe, Phys. Rev. B **71**, 035211 (2005).
[21] D. W. Brenner, Phys. Rev. B **42**, 9458 (1990).
[22] H. U. Jäger and K. Albe, J. Appl. Phys. **88**, 1129 (2000).
[23] H. U. Jäger and A. Y. Belov, Phys. Rev. B **68**, 024021 (2003).
[24] E. Neyts, A. Bogaertsa, R. Gijbelsa, J. Benediktb, and M. C. M. van de Sandenb, Diamond Relat. Mater. **13**, 1873 (2004).
[25] E. Neyts, A. Bogaerts, and M. C. M. van de Sanden, J. Appl. Phys. **99**, 014902 (2006).
[26] A. Y. Belov, Comput. Mater. Sci. **27**, 30 (2003).
[27] M. Moseler, P. Gumbsch, C. Casiraghi, A. C. Ferrari, and J. Robertson, Science **309**, 1545 (2005).
[28] D. W. Brenner, O. A. Shenderova, J. A. Harrison, S. J. Stuart, B. Ni, and S. B. Sinnott, J. Phys.: Condens. Matter **14**, 783 (2002).
[29] S. B. Sinnott, R. J. Colton, C. T. White, O. A. Shenderova, D. W. Brenner, and J. A. Harrison, J. Vac. Sci. Technol. A **15**, 936 (1997).
[30] S. J. Stuart, A. B. Tutein, and J. A. Harrison, J. Chem. Phys. **112**, 6472 (2000).
[31] S. J. Stuart, M. T. Knippenberg, O. Kum, and P. S. Krstic, Phys. Scr., T **24**, 58 (2006).
[32] J. Marian, L. A. Zepeda-Ruiz, N. Couto, E. M. Bringa, G. H. Gilmer, P. C. Stangeby, and T. D. Rognlien, J. Appl. Phys. **101**, 044506 (2007).
[33] N. A. Marks, Phys. Rev. B **63**, 035401 (2000).
[34] N. A. Marks, J. Phys.: Condens. Matter **14**, 2901 (2002).
[35] G. Opletal, T. Petersen, B. O'Malley, I. Snook, D. G. McCulloch, and N. A. Marks, Mol. Simul. **28**, 927 (2002).
[36] N. A. Marks, Diamond Relat. Mater. **14**, 1223 (2005).
[37] S. Izumi, S. Hara, T. Kumagai, and S. Sakai, Comput. Mater. Sci. **31**, 279 (2004).
[38] M. I. Baskes, Phys. Rev. B **46**, 2727 (1992).
[39] M. I. Baskes, Mater. Sci. Eng., A **261**, 165 (1999).
[40] M. I. Baskes, Mater. Chem. Phys. **50**, 152 (1997).
[41] C. J. Wu, Phys. Rev. Lett. **89**, 135701 (2002).
[42] W. L. Jorgensen, J. Phys. Chem. **87**, 5304 (1983).
[43] D. S. Franzblau, Phys. Rev. B **44**, 4925 (1991).
[44] G. Kresse and J. Hafner, Phys. Rev. B **47**, 558 (1993).
[45] G. Kresse and J. Furthmüller, Phys. Rev. B **54**, 11169 (1996).
[46] J. P. Perdew and Y. Wang, Phys. Rev. B **45**, 13244 (1992).
[47] J. P. Perdew, K. Burke, and M. Ernzerhof, Phys. Rev. Lett. **77**, 3865 (1996).
[48] P. E. Blöchl, Phys. Rev. B **50**, 17953 (1994).
[49] G. Kresse and D. Joubert, Phys. Rev. B **59**, 1758 (1999).
[50] P. J. Fallon, V. S. Veerasamy, C. A. Davis, J. Robertson, G. Amaratunga, W. I. Milne, and J. Koskinen, Phys. Rev. B **48**, 4777 (1993).
[51] S. Ravi, P. Silva, Shi Xu, B. X. Tay, H. S. Tan, and W. I. Milne, Appl. Phys. Lett. **69**, 491 (1996).
[52] K. W. R. Gilkes, P. H. Gaskell, and J. Robertson, Phys. Rev. B **51**, 12303 (1995).
[53] *Chemical Handbook (Kagaku-Binran)*, 5th ed., edited by The Chemical Society of Japan (Maruzen, Tokyo, 2004).
[54] J. Bernholc, A. Antonelli, T. M. Del Sole, Y. Bar-Yam, and S. T. Pantelides, Phys. Rev. Lett. **61**, 2689 (1988).
[55] E. Kaxiras and K. C. Pandey, Phys. Rev. Lett. **61**, 2693 (1988).
[56] O. L. Blakslee, D. G. Proctor, E. J. Seldin, G. B. Spence, and T. Weng, J. Appl. Phys. **41**, 3373 (1970).
[57] M. T. Yin and M. L. Cohen, Phys. Rev. Lett. **50**, 2006 (1983).